Quantitative Ultrasound Spectroscopy for the Estimation of Cellular Structures using the Structure Factor Model

P. Muleki-Seya, R. Guillermin, F. Tourniaire, **E. Franceschini**
Laboratoire de Mécanique et d'Acoustique LMA - CNRS UPR 7051, Aix-Marseille University, Centrale Marseille, Marseille, France
Phone : 04 84 52 42 86, Email: franceschini@lma.cnrs-mrs.fr

J. Guglielmi, T. Pourcher
Laboratoire TIRO, UMRE 4320, iBEB, DSV, CEA, University of Nice Sophia Antipolis, Nice, France

J. Chen and E. Konofagou
Department of Biomedical Engineering and Radiology, Columbia University, New York, NY, USA

J. Mamou
F. L. Lizzi Center for Biomedical Engineering, Riverside Research, New York, NY, USA

Key words : Quantitative Ultrasound, spectroscopy, structure factor, cellular structure

1 INTRODUCTION

1.1 Clinical motivation

Clinical ultrasound imaging such as echography is the most frequently used imaging modality in the world accounting for almost 25% of all imaging procedures (Forsberg 2004). In the field of cancer imaging, the role of ultrasound imaging is primarily to differentiate solid tumors from cysts and to guide needle and surgical excision biopsies. Sonography is very useful for locating lesions and ruling out cysts, although the definitive differential diagnosis requires pathological analysis of biopsy samples. The optical observation of the biopsy samples allows to observe the tissue and cell organization and cytoarchitectural features to determine the tumor benignancy or malignancy. Our goal is to increase the diagnostic information provided by ultrasound scans non-invasively and at low cost to reduce the number of questionable biopsies without sacrificing diagnostic performance. Such methods can be used periodically for the initial diagnosis and regularly for monitoring a patient's response to treatment.

1.2 Ultrasound and tissue structure estimation

Despite the safety and popularity of ultrasound imaging, relatively unsophisticated pulse echo techniques are still the basis of this modality, resulting in a qualitative imaging where the gray level is not related to significant parameters of the medium. Conventional echographic images are constructed from envelope-detected Radio Frequency (RF) signals that are backscattered. The RF echoes are created by reflections from interfaces between acoustically different regions (macrostructure). Conventional echographic images display large-scale structures (greater than wavelength), but to quantify and display smaller scale structures (smaller than wavelength), the frequency-dependent echo data must be utilized and related to physical parameters. Unfortunately, the conventional image formation process removes this frequency-dependent information. Ultrasound backscatter spectroscopy aims to estimate local tissue acoustic parameters through analysis of the frequency (spectral) content of backscattered signals, which are related to the tissue microstructure (Lizzi *et al.* 1986).

For years, many investigators have attempted to estimate the tissue structure properties (i.e. scatterer size and concentration) by analyzing the power spectra of the radio frequency (RF) data. The access to RF data from laboratory instruments and, increasingly, from clinical scanners allows application of a normalization procedure (Madsen *et al.* 1984, Wang & Shung1997) to obtain the backscattering coefficient (BSC), defined as the power backscattered by a unit volume of scatterers per unit incident intensity per unit solid angle. Thanks to this normalization procedure, the BSC is an experimental measure independent from the instrumental function. The aim of the present article is to provide a review with emphasis on Quantitative UltraSound (QUS) techniques to extract tissue structure parameters that relies on theoretical scattering models to predict the BSC.

2 STATE OF THE ART : ULTRASOUND SCATTERER SIZE IMAGING

A class of QUS techniques consist in fitting the experimental BSC from biological tissues to a theoretical BSC derived using an appropriated scattering model (Insana *et al.* 1990). The fit parameters can provide a meaningful description of the tissue microstructure (e.g., scatterer size, shape, scattering strength, spatial organization, etc.) provided that the chosen scattering model is accurate for the tissue under investigation. One of the most popular scattering models is the spherical Gaussian model (SGM) developed by Lizzi *et al.* (1986). This model describes tissue as a random medium composed of spherical structures having continuous spherical impedance fluctuation following a spherical Gaussian curve. One of the key features of the SGM is that fitting is computationally efficient (Oelze *et al.* 2002) and yields two QUS estimates describing tissue microstructure : the average effective scatterer size and the so-called acoustic concentration (i.e., the product of the scatterer number density and the square of the relative impedance difference between the scatterers and the surrounding medium). A second class of theoretical scattering models describes tissue as an ensemble of discrete scatterers with an impedance differing from a homogeneous background medium, where the cells are generally considered as the dominant source of scatterers and modeled as fluid-filled spheres, called the Fluid-Filled Sphere Model (FFSM) (Oelze & O'Brien 2006). This section describes the SGM and the FFSM, as well as some examples of QUS estimations based on these models.

2.1 Ultrasound sparse scattering models : the Spherical Gaussian model (SGM) and the Fluid-Filled Sphere Model (FFSM)

In the following, it is assumed that the wavelength is large in comparison with small diffuse structures inside the tissue under investigation. Modeling tissue as a viscous fluid containing randomly positioned scattering sites, one can adopt a statistical description of the cellular-scale structures. The reader can refer to the book chapter of Insana and Brown(1993) to have a complete course on acoustic scattering theory applied to soft tissues. A short summary is given here.

To model ultrasound backscattering by soft tissues, some simplifying assumptions (but nevertheless acoustically realistic) are necessary. It is assumed that :
- The scatterers are insonified by a plane wave, locally, in the region-of-interest under investigation
- Shear wave propagation and wave mode conversion are neglected such that only compressional waves are taken into account.
- The scattered wave is small in comparison to the incident wave (Born approximation), such that multiple scattering is neglected. This requires that the acoustic parameters between the scatterers and the surrounding medium be small.
- The medium is isotropic random.

By considering an ensemble of identical scatterers of radius a that are randomly and independently distributed (where the volume fraction of scatterers is typically less than a few percents), each scattterer equally and individually contributes to the backscattered power. The BSC is thus proportional to the average number of scatterers per unit volume n (also called the scatterer number density related to the volume fraction ϕ as $n = \phi/V_s$ where V_s is the scatterer volume). The theoretical BSC can be expressed as the product of the BSC in the Rayleigh limit and the backscatter form factor FF as follows (Insana and Brown 1993) :

$$\begin{aligned} BSC_{\text{sparse}}(k) &= n\sigma_b(k,a)FF(k,a) \\ &= n\frac{k^4 V_s^2 \gamma_z^2}{4\pi^2} FF(k,a) \end{aligned} \quad (1)$$

where k is the wavenumber and γ_z is the relative acoustic impedance difference between scatterers and the surrounding tissue $\gamma_z = \frac{z - z_0}{z_0}$. The differential backscattering cross section of a single scatterer in the Rayleigh limit σ_b depends on the fourth power of the ultrasound frequency and vary as the square of the scatterer volume. Form factors FF are functions that describe the amplitude of the backscattered intensity due to a single scattering structure as a function of frequency (or equivalently, as a function of the wave vector amplitude k). The form factors are based on 3D spatial correlation models by assuming some form or shape for the scattering tissue structures. Usually simple scattering shapes are assumed and in most cases they have a spherical symmetry. Commonly used form factors include the fluid sphere or the Gaussian. The fluid sphere form factor FF_{FS} assumes that the scatterer is a homogeneous sphere filled with a fluid, whereas the spherical Gaussian form factor FF_{SG} hypothesizes a continuous Gaussian distribution with spherical symmetry of relative impedance between the scatterer and the

surrounding medium. So, in the case of the SGM, the radius a corresponds to an effective scatterer radius. The form factors are defined as :

$$\begin{aligned} FF_{\text{FS}}(k,x) &= \left[\frac{3}{(2ka)^3} j_1(2ka)\right]^2 \quad \text{(fluid sphere)}, \\ FF_{\text{SG}}(k,x) &= e^{-0.827k^2a^2} \quad \text{(Gaussian)}, \end{aligned} \tag{2}$$

where j_1 is the spherical bessel function of the first kind of order 1.
Both models yields two tissue properties : the average scatterer size a and the acoustic concentration $n_z = n\gamma_z^2$. Note that the scatterer size could be determined using the frequency dependence of the form factor as performed previously by Oelze (2002). Some example of predicted theoretical BSC are given in Fig. 1(a). Estimated values of a^* and n_z^* are determined by fitting the measured BSC to the theoretical SGM or FFSM.

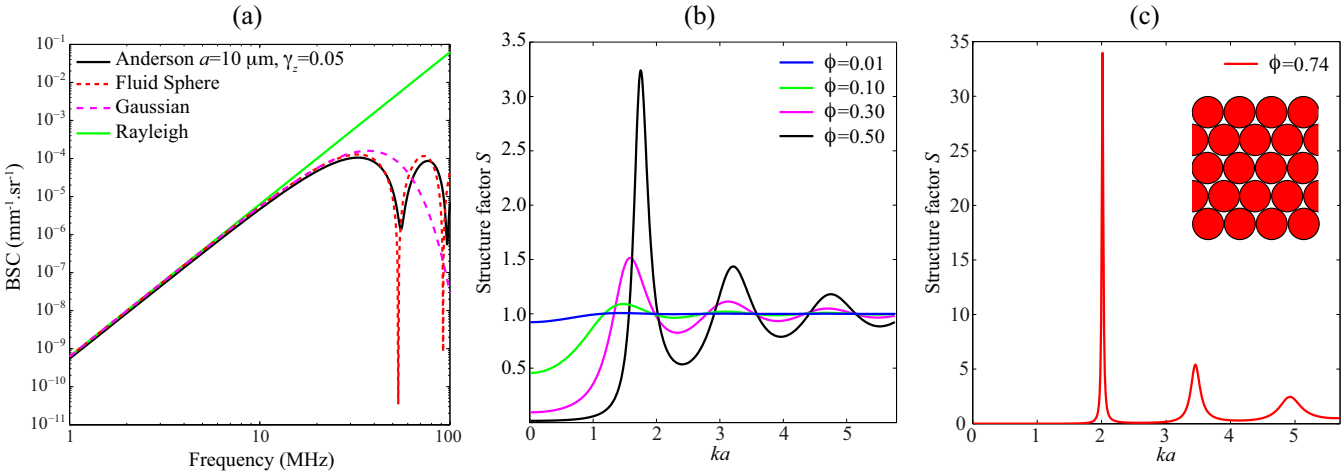

FIGURE 1 – (a) Example of theoretical frequency-dependent BSC for a sphere of radius 10 μm and impedance contrast of 0.05 calculated using the exact Anderson model (Anderson 1950), the FFSM and the SGM. Also represented is the response from an ensemble of Rayleigh scatterers. (b) and (c) Structure factor curves as a function of product ka for several volume fractions of 0.01, 0.10, 0.30, 0.50 and 0.74.

2.2 Ultrasound scatterer size from tissues : successes and limits

The goal of QUS is to associate these QUS parameter values with specific tissue structures (Lizzi *et al.* 1986). Feleppa *et al.* (1986, 1996) demonstrated that the effective scatterer size was relevant to detect ocular or prostate tumors. In ocular malignant tumors, larger scatterer sizes were estimated by ultrasound when compared to normal tissues and were related to clusters of melanin-laden histiocytes [2]. Waag *et al.* (1983) related the ultrasound backscatter measurements to the lobule structures in the liver. Oelze *et al.* (2004) distinguished fibroadenoma (benign tumors) and carcinoma (malignant tumors) based on the QUS estimates. The scatterer-size QUS images showed that the fibroadenoma have larger scatterers that correspond to the glandular acini sizes and that carcinoma have smaller, more uniform scatterer sizes (Oelze *et al.* 2004).

However, it is often difficult to establish a relationship between QUS scatterer properties estimates and tissue microstructure identified from optical microscope images (Oelze & O'Brien 2006, Han *et al.* 2011). This difficulty may originate from an unsuitable modeling of the individual scatterers when using the classical form factors ; *i.e.*, the Gaussian or the fluid sphere form factors. Interest has thus grown in developing new modeling for the individual cell by considering a more complete description of the individual cell. Oelze & O'Brien (2006) developed a new cell model to consider backscattering from cell nuclei and cytoskeleton using the autocorrelation function of the 3D spatial mapping of the cell impedance. The SGM, the FFSM and the new cell model were compared to examine two mouse models of mammary cancers : carcinoma with a uniform distribution of cells and sarcoma with clusters of cells. None of the three models produced good fits to the data, and QUS estimates did not faithfully represent the actual microstructural differences as observed from histological images (Oelze

& O'Brien 2006). Han *et al* (2011) developed cell pellet biophantoms that consist of identical cells embedded in a plasma-thrombin supportive background with various cell concentrations ranging from 0.17% to 63%. The concentrated biophantoms mimic densely packed cells with controlled cell volume fractions and are simplified versions of real tissue since only a single cell line is considered. The BSC estimates from the biophantoms were fitted with two concentric fluid spheres theory (McNew *et al.* 2009) in a large frequency bandwidth from 26 to 105 MHz. At low cell volume fractions ($\leq$0.026), the estimated whole cell radii agree well with the true whole cell radii, but not at high cell volume fractions ($>$0.096) (Han *et al.* 2011). These results suggest that the two concentric fluid spheres theory used to obtain the QUS estimates might be inappropriate.

Another reason that could explain the difficulty to correlate the cellular structures estimated by ultrasound and obtained from histological observations may be an unsuitable modeling for an ensemble of cells. In the aforementioned models (SGM, FFSM, new cell model and concentric sphere model), the scatterers are assumed to be independently and randomly distributed (*i.e.,* to have a low scatterer volume fraction). Under this hypothesis, the power of the backscattered signals increases linearly with the scatterer volume fraction and depends on the size and acoustic properties of the tissue scattering structures. This linear relationship has been used to monitor the scatterer size and/or acoustic concentration. However, the assumption of randomly distributed scatterers may not hold in concentrated cell pellet biophantoms (Han *et al.* 2015) or in tumors with densely packed cells (Vlad *et al.* 2010). Therefore, our hypothesis is that a scattering model considering the interference effects caused by the correlation among scatterer positions (*i.e.* considering the coherent scattering) may help to estimate QUS parameters and to reveal the absolute cellular structures of the tissue, as described in the next section 3.

3 ON THE USE OF A CONCENTRATED SCATTERING MODEL : THE STRUCTURE FACTOR MODEL FOR CHARACTERIZING TISSUES

This section introduces the concentrated scattering model, namely the Structure Factor Model (SFM), and the recent advances in the QUS cellular structure estimation based on this modeling.

3.1 The Structure Factor Model (SFM)

The SFM is based on the assumption that at high scatterer concentrations, interference effects are mainly caused by correlations between the spatial positions of individual scatterers. The SFM considers the coherent scattering by summing the contributions from individual cells and modeling the cellular interaction by a statistical mechanics structure factor (Twersky 1987, Savery & Cloutier 2001). In comparison with the classical described in Eq. (1), the SFM considers the interference effects relatively easily by replacing the single-particle backscattering contribution $\sigma_b(k,a)$ by the product $\sigma_b(k,a)S(k,a,\phi)$, where $S(k,a,\phi)$ is the structure factor depending on the scatterer concentration ϕ and the pattern of the spatial arrangement of the scatterers. By considering an ensemble of identical fluid spheres of radius a, the theoretical BSC for the SFM formulation is given by :

$$BSC_{\text{SFM}}(k) = m\sigma_b(k,a)FF_{\text{FS}}(k,a)S(k,a,\phi), \tag{3}$$

where the differential backscattering cross section σ_b is calculated using the spherical form factor FF_{FS}. Note that there is no simple analytical expression of the structure factor for a complex spatial positioning of particles. However, for an ensemble of identical hard (i.e. non deformable) spheres that are homogeneously distributed, the structure factor depends on the sphere radius and the sphere concentration, and its analytical expression can be obtained as established by Wertheim (1963). The structure factor has an influence on the BSC frequency dependency and amplitude, as observed by plotting the structure factor versus the product ka in Fig. 1(b) and (c). For example, in the case of a sphere concentration of 0.30, the structure factor ranges between 0.10 and 1 for ka ranging between 0 and 1.

3.2 Experiments and results

Several studies were conducted at high frequencies to examine the capabilities and limitations of ultrasonic tissue structure estimation based on the SFM. Franceschini & Guillermin (2012) performed experiments on tissue-mimicking phantoms to show the superiority of the SFM in comparison with other classical models that do not account for the structure factor (*i.e.,* the SGM and the FFSM) to

explain the BSC behavior for concentrated media. Experiments were also conducted on cell pellet biophantoms mimicking densely packed cells, on *ex vivo* canine livers and on *ex vivo* solid tumors in mice and allowed us to investigate the SFM capabilities.

First, cell pellet biophantoms were examined (Franceschini *et al.* 2014, 2016). These biophantoms consisted of human leukemia K562 cells trapped in a mixture of plasma and thrombin with different cellular volume fractions ranging from 0.6% to 30%. Ultrasonic backscatter measurements were made from frequencies from 10 MHz to 42 MHz using an ultrasound scanner (Vevo 770, Visualsonics, Toronto, Canada) equipped with the RMV 710 and 703 probes. Two sparse models (SGM and SFM) and one concentrated model (SFM) were investigated to estimate scatterer size and acoustic concentration. Results are reported in Fig. 2. The SGM and the FFSM give satisfactory estimates for the lowest volume fractions ($\phi_c \leq 6\%$), but for the highest volume fractions, $\phi_c > 6\%$, they underestimate the cellular size and overestimate the acoustic concentration. One can notice that the radius estimated by the classical models decreases as the cellular volume fraction increases, whereas the radius is generally estimated around 8.18μm when using the SFM, whatever the studied volume fraction. Only the SFM gives satisfactory estimates for both structural parameters (radius and acoustic concentration).

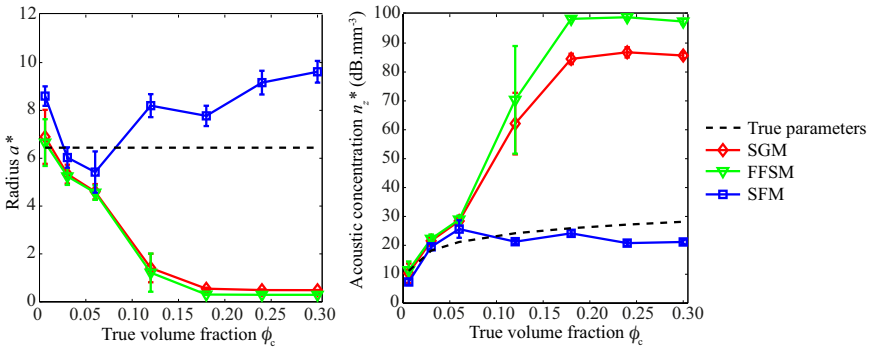

FIGURE 2 – Radius a^* and acoustic concentration $(n_z)^*$ estimated by the three scattering models (SGM, FFSM and SFM).

Secondly, excised canine livers were scanned with a 25 MHz transducer (Muleki *et al.* 2016). The liver was chosen because of its relative homogeneity compared to other tissue. Scatterer size a^* and acoustic concentration n_z^* averaged for all the canine livers are reported in Fig. 3. The scatterer radius a^* and the acoustic concentration n_z^* obtained from the FFSM, SGM and SFM are quasi-identical. This result was obtained previously with the diluted cell pellet biophantoms experiments for cell volume fractions less than 0.06. Indeed, when the medium is diluted, the structure factor is closed from the unity value (as shown in Fig. 1), and the SFM is reduced to the FFSM modeling. So the similar QUS estimates obtained with the sparse models (SGM and FFSM) and the concentrated model (SFM) suggest that the liver is a diluted medium (with low scatterer volume fraction). Moreover, the three models (SGM, FFSM and SFM) give a mean scatterer radius around 5.26 μm that closely matched the true radius of hepathocyte nuclei with a relative error around 8%. These findings corroborate also the diluted medium consideration. Indeed, if the nuclei (and not the whole cells) are the cellular structures responsible for scattering, the corresponding scatterer volume fraction was expected to be small (approximately 0.02). To conclude, the QUS parameter estimates with the three scattering models show that the nucleus is the dominant source of scattering in the liver. This conclusion was suggested previously in a numerical study based on 3D impedance maps of rabbit liver (Pawlicki *et al.* 2011).

Thirdly, colon adenocarcinoma (HT29) mouse models were examined with a 30 MHz transducer (Muleki *et al.* 2016). Human colon adenocarcinoma HT29 cell line were cultured in medium and then injected subcutaneously into the flank of 6- to 8-week old Nude mice. After two or three weeks of growth, tumors were excised and examined using ultrasound cellular structure imaging. Scatterer size

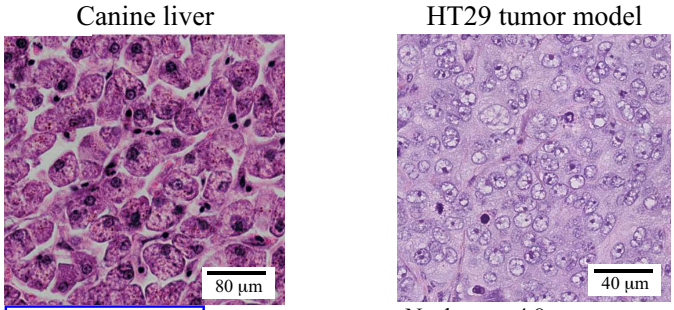

	a (µm)	n_z (dB.mm^{-3})
SFM	5.34	26.58
FFSM	5.18	26.50
SGM	5.28	26.07

Frequency bandwidth 10-38 MHz

	a (µm)	n_z (dB.mm^{-3})
SFM	7.24	33.05
FFSM	1.15	83.75
SGM	0.94	84.18

Frequency bandwidth 15-42 MHz

FIGURE 3 – Top row : Examples of histological images of a canine liver (on the left) and of a HT29 mouse tumor (on the right), and corresponding mean nucleus and whole cell radii deduced from the optical images. Bottom row : Mean estimated values of a^* and n_z^* obtained with the SFM, FFSM and SGM for the canine livers (on the left) and for the HT29 mouse tumors (on the right).

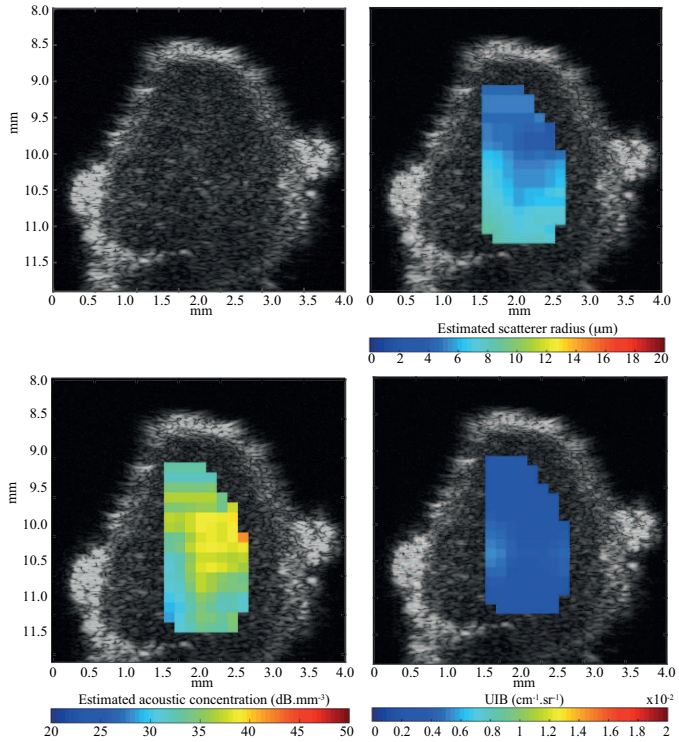

FIGURE 4 – Quantitative images using the SFM for a homogeneous tumor superimposed on the gray-scale B-mode image.

a^* and acoustic concentration n_z^* averaged for all the mouse tumors are reported in Fig. 3. Figure 4 shows an example of QUS parameters estimated with the SFM, as well as the Ultrasound Integrated Backscatter (UIB) parameter. The scatterers radius a^*, acoustic concentration n_z^* and UIB images were constructed by superimposing color-coded pixels on a conventional gray-scale B-mode image of the tumors. The size and location of the color-coded pixels corresponded to regions-of-interest from which parameters estimates were obtained. The mean scatterer radius estimated with the SFM was found equal to 7.24 μm, which corresponds quite well to the true whole HT29 cell radius of 6.71 μm with relative errors of 8%. The mean scatterer radius obtained with the SGM and FFSM are equal to 1.15

and 0.94 μm. So the QUS parameters estimated with the sparse models are not correlated with the cellular structures. Large differences in the QUS parameter estimates were obtained depending upon the use of sparse or concentrated model. In experiments on cell pellet biophantoms, it has been previously observed that the sparse models underestimated scatterer size and overestimated acoustic concentration when the volume fraction was greater than 6%. The same behavior was obtained in the present study on *ex vivo* mouse tumors demonstrating that the HT29 tumors could be consider as concentrated media with densely packed cells. These findings suggest the whole HT29 cell is the dominant source scattering in the HT29 mouse tumors.

4 PERSPECTIVES IN THE FIELD OF QUANTITATIVE ULTRASOUND TECHNIQUES

In summary, the experimental studies presented in section 3 demonstrated the satisfactory performance of the SFM even in the case of sparse media. Therefore, the methods described here could be used to interpret QUS estimates of tissue microstructure with better accuracy. Our hypothesis is that the QUS parameters obtained from the SFM are physically correct and can, therefore, be correlated to the true tissue structure. Histology images of tumors and tissues in general often show densely packed cells and so we can reasonably assume that the SFM is a more-appropriate model to use for modeling densely packed cellular content in tumors and a wide range of other tissues. The QUS estimates derived from the SFM could better characterize tissue types and prove invaluable for assessing disease or monitoring treatment *in vivo* using clinical ultrasound systems.

The experimental studies proposed here focus on quite homogeneous tissue or tumor. However, tumors have more complex structures. The extracellular matrix, the blood microvessels and the tumor heterogeneity (with proliferating and necrotic cell type regions) may play a role in tumor backscatter. In the HT29 animal model, some tumors that are allow to grow large enough develop a necrotic core (Muleki *et al.* 2016). In this necrotic area, QUS parameter estimates with the SFM were difficult to interpret and to correlate with the true cellular structures observed in histological images because of the presence of two areas : a cellular area containing viable HT29 tumor cell and a necrotic area containing a majority of Natural Killer (NK) lymphocytes and no viable tumor cells. At the moment, the SFM is an improvement over the sparse scattering models (SGM and FFSM) for modeling high cellular content in simple tumor/tissue composed of a single cell line. Future work should focus on taking into account the heterogeneity of cell types as well as other structures such as blood microvessels.

Finally, the appropriate frequency bandwidth for using the SFM is approximately at a product ka around 1. Considering that cell radii are around 5-8 μm, high frequencies (20-40 MHz) are thus required. Due to tissue attenuation, the approach would be limited to superficial cancers (*i. e.*, ocular, thyroid, prostate, skin and superficial breast tumors). But developments in transducer technology may soon permit high frequency transducers to be mounted on catheters that can be used to image deep-seated tumors.

REFERENCES

Anderson V. C. , “Sound scattering from a fluid sphere", *J. Acoust. Soc. Am.* **22**, (1950), pp. 426-431

Feleppa E. J. , Lizzi F. L. , D. J. Coleman, and M. M. Yaremko, “Diagnostic spectrum analysis in ophthalmology : a physical perspective", *Ultrasound Med. Biol.* **12**, (1986), pp. 623-631

Feleppa E. J. , Kalisz A., Sokil-Melgar J. B. , Lizzi F. L. , Liu T., Rosado A. L. , Shao M. C. , Fair W. R. , Wang Y., Cookson M. S. , Reuter V. and Heston W. D. W. , “Typing of prostate issue by ultrasonic spectrum analysis", *IEEE Trans. ultras. Ferroelectr. Freq. Control.* **43**, (1996), pp. 609-619

Forsberg F., “Ultrasonic biomedical technology ; marketing versus clinical reality", *Ultrasonics* **42**, 1-9, (2004), pp.17-27

Franceschini E. and Guillermin R., “Experimental assessment of four ultrasound scattering models for characterizing concentrated tissue-mimicking phantoms", *J. Acoust. Soc. Am.* **132**, (2012), pp.3735-3747

Franceschini E., Guillermin R., Tourniaire F., Roffino S., Lamy E. and Landrier J.-F. , “Structure Factor Model for understanding the measured backscatter coefficients from concentrated cell pellet biophantoms", *J. Acoust. Soc. Amer.* **135**, (2014), pp. 3620-3631

Franceschini E., de Monchy R. and Mamou J., “Quantitative characterization of tissue microstructure on concentrated cell pellet biophantoms based on the structure factor model", submitted to IEEE Trans. ultras. Ferroelectr. Freq. Control. special issue on Quantitative Ultrasound-Based Tissue Characterization (2016)

Han A., Abuhabsah R., Blue J. P., Sarwate S. and O'Brien W. D., "Ultrasonic backscatter coefficient quantitative estimates from high-concentration Chinese hamster ovary cell pellet biophantoms", *J. Acoust. Soc. Am.***130**, (2001), pp. 4139-4147

Han A. and O'Brien W. D. , "Structure function for high-concentration biophantoms of polydiperse scatterer sizes", *IEEE Trans. ultras. Ferroelectr. Freq. Control.* **62** (2015), pp. 303-318

Insana M. F., Wagner R. F., Brown D. G. and Hall T. J., "Describing small-scale structure in random media using pulse-echo ultrasound", *J. Acoust. Soc. Am.* **87**, (1990), pp. 179-192

Insana M. F. and Brown D. G., "Acoustic scattering theory applied to soft biological tissues", in *Ultrasonic Scattering in Biological Tissues*, edited by K. K. Shung and G. A. Thieme (CRC, Boca Raton, FL, 1993), Chap.4, pp. 76-124.

Lizzi F. L., Ostromogilsky M., Feleppa E. J., Rorke M. C., and Yaremko M. M., "Relationship of ultrasonic spectral parameters to features of tissue microstructure", *IEEE Trans. Ultrason. Ferroelect. Freq. Contr.* **33** (1986), pp. 319-329

Madsen E. L., Insana M. F. and Zagzebski J. A., "Method of data reduction for accurate determination of acoustic backscatter coefficients", *J. Acoust. Soc. Am.* **76** (1984), pp. 913-923

Muleki-Seya P., Guillermin R., Guglielmi J., Chen J., Pourcher T., Konofagou E. and Franceschini E., "High frequency quantitative ultrasound spectroscopy of excised canine livers and mouse tumors using the structure factor model", submitted to IEEE Trans. ultras. Ferroelectr. Freq. Control. special issue on Quantitative Ultrasound-Based Tissue Characterization (2016)

McNew J., Lavarello R. and OâĂŹBrien W. D., "Sound scattering from two concentric fluid spheres (L)", *J. Acoust. Soc. Am.* **125**, (2009), pp. 1-4

Oelze M. L. , Zachary J. F. and O'Brien W. D. , "Characterization of tissue microstructure using ultrasonic backscatter : Theory and technique for optimization using a Gaussian form factor", *J. Acoust. Soc. Am.* **112**, (2002), pp. 1202-1211

Oelze M. L. , O'Brien W. D., Blue J. P., and Zachary J. F., "Differentiation and characterization of rat mammary fibroadenomas and 4T1 mouse carcinomas using quantitative ultrasound imaging", *IEEE Trans. Med. Imaging* **23**, (2004), pp. 764-771

Oelze M. L. and O'Brien W. D., "Application of three scattering models to characterization of of solid tumors in mice", *Ultrasonic Imaging* **28**, (2006), pp. 83-96

Pawlicki A. D., Dapore A. J., Sarwate S. and O'Brien W. D., "Three-dimensional impedance map analysis of rabbit liver", *J. Acoust. Soc. Amer.* **130**, (2011), pp. EL334-338

Savery D. and Cloutier G., "A point process approach to assess the frequency dependence of ultrasound backscattering by aggregating red blood cells", *J. Acoust. Soc. Am.* **110**, (2001), pp. 3252-3262

Twersky V., "Low-frequency scattering by correlated distributions of randomly oriented particles", *J. Acoust. Soc. Am.* **81**, (1987) pp. 1609-1618

Vlad R. M. , Saha R. K. , Alajez N. M., Ranieari S., Czarnota G. J. and Kolios M. C. , "An increase in cellular size variance contributes to the increase in ultrasound backscatter during cell death", *Ultrasound in Medicine & Biology* **9**, (2010), pp. 1546-1558

Waag R. C. , Nilsson J. O. and Astheimer J. P., "Characterization of volume scattering power spectra in isotropic media from power spectra of scattering by planes", *J. Acoust. Soc. Am.* **74** 1983), pp. 1555-1571

Wang S. H. and Shung K. K., "An approach for measuring ultrasonic backscattering from biological tissues with focused transducers", *IEEE Trans. Biomed. Eng.* **44** (1997), pp. 549-554